Geophys. J. R. astr. Soc. (1978) **55**, 67–86

Statistical study of the occurrence of shallow earthquakes

Yan Kagan and Leon Knopoff *Institute of Geophysics and Planetary Physics, University of California, Los Angeles, California 90024, USA*

Received 1978 January 17; in original form 1977 July 5

Summary. The time–space–magnitude interaction of shallow earthquakes has been investigated for three catalogues: worldwide ($M \geqslant 7.0$), Southern and Northern California ($M \geqslant 4.0$) and Central California ($M \geqslant 1.5$). The earthquake sequences are considered as a multi-dimensional stochastic point process; the estimates of the parameters for a branching model of the seismic process are obtained by a maximum-likelihood procedure. After applying magnitude–time and magnitude–distance scaling, the pattern of relationship among earthquakes of different magnitude ranges is almost identical. The number of foreshocks diminishes as the magnitude difference between the main shock and the foreshocks increases, while the magnitude distribution of aftershocks has the opposite property. The strongest aftershocks are likely to occur at the beginning of the sequence; later they migrate away with velocities of the order of km/day. The sequences which are composed of smaller aftershocks last longer and there are indications that they remain essentially in the focal region. Foreshocks also appear to migrate, but in this case, toward the main shock. The rate of occurrence of dependent shocks increases as t^{-1} as the origin time of the main shock is approached, effectively making every earthquake a multi-shock event. This interaction of earthquakes was modelled by a Monte-Carlo simulation technique. The statistical inversion of simulated catalogues was undertaken to derive the information we would be able to retrieve from actual data, as well as possible errors of estimates. The possibility of using these results as a tool for seismic risk prediction is discussed and evaluated.

1 Introduction

This paper is a continuation of our efforts to investigate the interaction among earthquakes using statistical methods (Kagan & Knopoff 1976; Kagan & Knopoff 1977; hereinafter I and II respectively). In I a stochastic model of time–space–magnitude interrelationships among earthquakes was proposed and some properties of the seismicity of strong earthquakes was studied. In II we discussed the possibility of making statistical predictions of

earthquakes, and evaluated the predictability of the seismic process of strong earthquakes. In I and II we used a corrected catalogue of large earthquakes ($M \geqslant 7.0$) (Duda 1965) extended to date, as raw data. This catalogue contains less than 1000 shallow shocks; the narrow magnitude span and the small size of this catalogue has prevented us from investigating some important problems of earthquake interaction, the answers to which are necessary for more accurate seismic risk calculations, as well as for understanding some aspects of the earthquake focal process. Some of these questions are: (1) Is seismicity self-similar for collections of earthquakes having remotely different magnitudes? (2) Are there significant differences in the time–distance–magnitude distributions for foreshocks and aftershocks? How is the major shock anticipated? What is the detailed history of seismicity after the earthquake? (3) How much information can be extracted from both local and global earthquake catalogues to permit the prediction of future seismic risk? To answer these questions we need much more complete and diverse data than those used in I and II.

In this paper we extend, with some modifications, the investigations made with the Duda catalogue to three available catalogues of California earthquakes: Southern California (Allen *et al.* 1965; Hileman, Allen & Nordquist 1973), Northern California (Bolt & Miller 1971, 1975) and Central California (Lee, Eaton & Brabb 1971; Lester, Kirkman & Meagher 1976 which also has references to earlier reports). These catalogues contain many thousands of earthquakes and are probably the best documented, most complete, and most accurate catalogues now in existence. Because of modifications of the procedure to be described below, we have also repeated the calculations for the Duda catalogue using the same model on all the catalogues.

2 The catalogues

In order to apply our statistical model (I) to an earthquake catalogue, certain conditions must be imposed, the most important of which is completeness of the catalogue. By this we mean that all, or almost all, the earthquakes within specified time–space–magnitude limits should be known. It is especially important that regular gaps of activity should not be present in the catalogues such as those, for instance, which might occur by omitting smaller shocks immediately after strong earthquakes; such gaps could easily introduce significant bias in the estimates of parameters and distortion of the calculated patterns of earthquake occurrence. A second condition is that the accuracy of hypocentre or epicentre determination be uniform for the entire catalogue. Because the distances between epicentres are used in the distance correlations (see I), the relative error of epicentre location is of concern to us; the distance errors should be essentially constant over space and time, i.e. for different parts of the area under investigation, as well as over the time span of the catalogue.

These requirements restrict the amount of earthquake data which is useful. Thus, in a given catalogue, many shocks are outside the 'uniform' region of space and time. We can use these latter earthquakes to try to reduce edge effects associated with neglect of the contribution of events outside the catalogue. We perform the suppression of edge effects by considering earthquakes outside the catalogue interval as main events which influence earthquakes inside the catalogue interval; on our model this would compensate for the lack of contribution from interactions between main shocks within the catalogue and dependent earthquakes outside it, since weaker events outside the catalogue are, in the main, absent. Of course, only those earthquakes outside the space and time region of the catalogue which interact with shocks inside, according to the model, will be taken into consideration.

What are the spans of homogeneity of space, time and magnitude of the catalogues? The catalogue which regularly reports the lowest magnitude shocks is the Central California

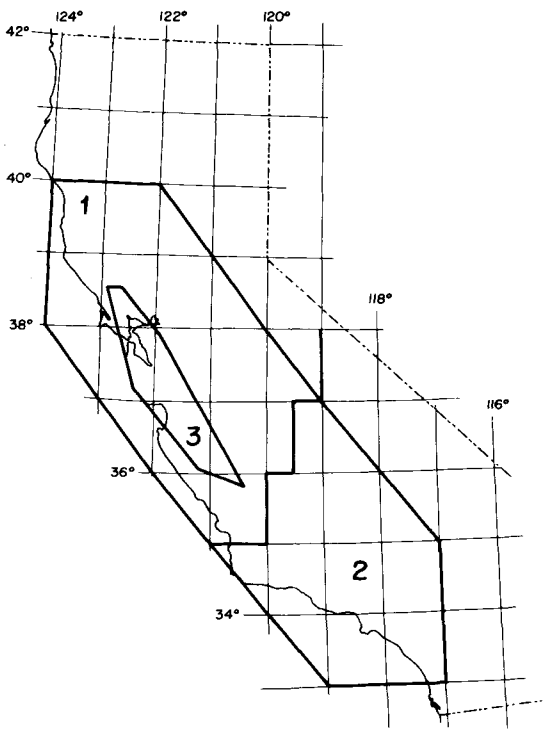

Figure 1. Map of California, showing the regions spanned by the catalogues: 1 – Northern California, 2 – Southern California, 3 – Central California (USGS).

catalogue prepared by the National Center for Earthquake Research (NCER), US Geological Survey. The NCER network consists of more than 100 stations in an area shown as region 3 in Fig. 1. The network began operation in 1969 and had roughly its present-day configuration after 1970; thus the time limits of our reduced catalogue have been taken as 1971–75. With regard to space limits, we have used the boundaries given by Lee *et al.* (1972b, fig. 1). These 1971 boundaries lie within enlarged perimeters given for later years (Lester *et al.* 1976, and earlier reports), but to ensure uniformity, we use the smaller region. The earthquakes within these boundaries are uniformly well located, i.e. spatial variations of standard errors for hypocentre locations are small in this area. As to the magnitude cutoff of the catalogue, although the lower limit of magnitudes may be as low as zero, coverage at this level is irregular; a more appropriate cutoff magnitude threshold is probably around $M = 1.0$. Magnitude–frequency plots of shocks inside the network area for each year in the interval 1969–75 are approximately parallel to each other down to magnitude 1.5; below this value, they are no longer linear and differ substantially from each other. Indeed, the plots for 1970 and 1971 show a decrease in the number of shocks below $M = 1.2$ or 1.3. As a further test, we compared the frequency distribution of two sets of earthquakes: (1) shocks which have epicentral distances less than 20 km from at least four stations, and (2) all the other shocks within the boundaries of the region. These distributions also appear to differ for $M \leqslant 1.5$. Of course, these differences may be caused by the irregular location of the stations in the network, or for geophysical reasons; as an example of the latter, variations in magnitude distributions before 1972 might have been associated with the Bear Valley earthquake of 1972 February 24 (Wesson & Ellsworth 1973). For reasons of caution, we use

earthquakes with $M \geqslant 1.5$ in our catalogue. In this case the catalogue contains 5689 'inside' earthquakes for 1971–75 and located within the boundaries of the region, and about 130 'outside' shocks, namely those from 1969–70 plus those located outside the boundaries of the region up to 1975. This catalogue is called USGS in this paper.

The second data set combines the Southern and Northern California catalogues. The catalogues available to us covered the periods from 1932 January 1 to 1975 December 31 for Southern California and from 1910 January 1 to 1974 June 30 for Northern California. During these time intervals the number of seismographic stations, recording equipment, methods of data processing and data presentation changed significantly. Thus the completeness and the uniformity of the catalogues is expected to be highly irregular. Both catalogues were combined to increase the total amount of data. The lower time limit for this combined catalogue was chosen to be 1944 January 1; before this date magnitudes were rounded off to the nearest half-unit, while in our computational model a round-off of 0.1 of a magnitude unit has been used (I). The upper time limit was taken to be 1974 June 30 from the mutual time span of both subsets. The spatial boundaries of the combined regions, thus defining the 'inside' region (Fig. 1), were selected to ensure roughly uniform coverage of the area by the seismic networks after 1944 (see above mentioned references and Gutenberg 1955). The magnitude limits are variable over the time interval between 1944 and 1974. Until the time of the Kern County Earthquake of 1952 July 21, the reliability threshold for the Southern California network was around $M = 4.0$ (Knopoff & Gardner 1969). During the Kern County aftershock sequence the cutoff magnitude remained about 4.0 for more than 100 days (Richter 1955). Subsequent to this earthquake an improvement in the instrumental density of the network lowered the threshold to about $M = 3.0$ (Knopoff & Gardner 1969). A significant increase in the density of stations in the Northern California network plus the start of a transition to computer techniques for locating epicentres began around 1961 (Bolt & Miller 1975). We have taken $M_L = 4.0$ as a magnitude threshold for the first part of the combined catalogue; from 1962 January 1 to the end of the catalogue we have used a magnitude threshold of $M_L = 3.5$. The combined California Catalogue (CACA) thus defined contains 997 events inside the interval and 246 events outside it.

With regard to the worldwide catalogue of large shallow earthquakes the Duda list (1965) forms the bulk of our catalogue; the lower magnitude limit is $M_s = 7.0$. We have extended this catalogue to 1975 April using the PDE data file (Meyers & von Hake 1976). As a lower time limit we have used 1905 January 1; before this date, listings of weaker events ($7.0 < M < 8.0$) are incomplete. 1972 December 31 was taken as the upper time limit. This catalogue (called DUDA below) contains 914 'inside' events and 81 'outside' events.

In the following discussion, a single magnitude scale is used which incorporates, without change of scale, both the M_s of DUDA and the M_L of CACA and USGS.

3 Moments

The second-order moments of a seismic process represent a convenient exploratory tool for studying interactions among earthquake events (I). In I we studied the conditional intensity function or conditional moment $m(x/x_1)$ of a seismic process, i.e. the number of earthquakes in a certain space–time interval x_1 given the occurrence of an earthquake at a point x. As raw data the DUDA catalogue was used. When we tried to apply a similar technique to the Southern California catalogue, we found that the seismic history of Southern California of the past 30 years is dominated by two large earthquakes: Kern County (1952) and San Fernando (1971). Thus a large number of the shocks listed in the catalogue are stochastically dependent on these earthquakes, and hence many of the events are statistically connected, although not necessarily directly.

The conditional time–distance moment will consist of contributions from both direct interactions and secondary interrelationships; the latter are represented by convolutions in the time–space domain of the former. The most interesting features of earthquake interactions are likely to be smoothed out by strong secondary interference effects in such convolutions. For now, we indicate that the second-order moments from the Southern California catalogue give approximately the same information as obtained from DUDA (I); below, we will return to this problem.

Before proceeding to the analysis of these catalogues using a stochastic model, we discuss the conditional spatial moment of the earthquake process. In I we found that the quantity $N(dr)/r$ is uniformly distributed over the distance range 200–2000 km for large worldwide earthquakes, where $N(dr)$ is the number of shocks in the distance interval between r and $r + dr$ from a given epicentre. We have checked whether the property of uniformity of this function applies to an earthquake process on a much smaller scale through the study of the earthquake catalogues for California. Catalogue USGS provides us with a unique opportunity to study the three-dimensional, or hypocentral, spatial moments, since it has estimates of focal depths which are probably as reliable as can be obtained routinely today. When we try to study the spatial distribution of USGS hypocentres we find that we must take into account edge effects due to boundaries of the region (see Fig. 1) and the non-uniform distribution of seismicity with depth: about one-half of all USGS earthquakes are concentrated in a depth interval 4 to 7 km. To take these effects into account we have first calculated the (conditional) number of USGS hypocentres $N(V_r)$, which are situated at distances less than r from a given earthquake. These computations were then repeated with a spatially randomized catalogue, where the same total number of shocks was distributed uniformly over the horizontal plane, but the depth distribution was taken to be the same as the USGS catalogue. The number of shocks in the simulated, i.e. Poissonian catalogue, for small distances $r < 3.2$ km, was too small for reliable comparison, but we can calculate these quantities, using the formula

$$N_p(V_r) = \frac{4\pi}{S}\int_0^r RdR \int_0^R K(h)\,dh$$

where the depth covariance function $K(h)$ is defined as

$$K(h) = \frac{1}{(\Delta z)^2}\int N(z, z + \Delta z) \cdot N(z + h, z + h + \Delta z)\,dz.$$

Here $N_p(V_r)$ is the number of pairs of hypocentres in a sphere of radius r centred on one shock focus; S is the surface area spanned by the USGS catalogue which is approximately, 19 200 km^2, $N(z, z + \Delta z)$ is the number of shocks in the depth interval $(z, z + \Delta z)$.

The ratio $N(V_r)/N_p(Vr)$ gives the spatial moment behaviour as if the shocks were distributed uniformly in all three directions. For display purposes this ratio is multiplied by r (Fig. 2). This product is essentially uniform over distances from 1 km to more than 20 km. For distances less than 1 km the hypocentre distribution is dominated by location errors; independent estimates of these errors are approximately 1 km, (Lee *et al.* 1971; Lester *et al.* 1976).

The increase in this curve (see Fig. 2) for $r > 20$ km is most probably connected with bias in choosing the regional boundaries of USGS with respect to the seismicity pattern. If, for example, we were to rotate the region of USGS so that its longer side is perpendicular to the San Andreas fault, the number of long-distance shocks would decrease significantly; a random orientation of the polygon would probably yield a uniform distribution of $r \cdot N(V_r)/N_p(V_r)$ over the entire long-distance range.

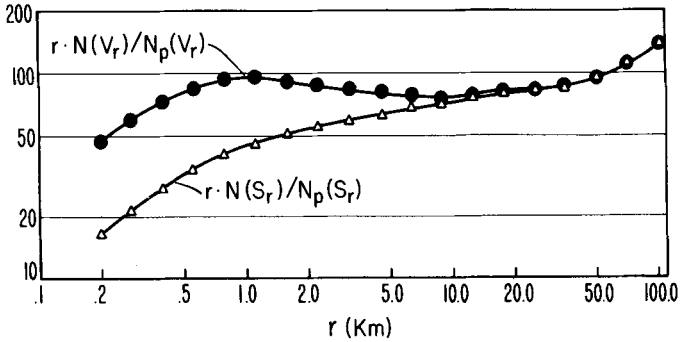

Figure 2. Spatial moments of the earthquake process.

Taking these considerations into account, we shall assume that the curve of spatial moment is proportional to r^{-1} over the entire range of distances. Since this result arose in I as well, we propose the conjecture that this is a general feature of the spatial distribution of earthquakes, pointing to some property of the geometry of faulting. For example, our conjecture rules out a spatially isotropic uniform distribution of earthquake faults. For the purposes of comparison of results later on, we have used only two-dimensional spatial moments in our calculations of the likelihood function for USGS, shown also in the lower curve in Fig. 2; in this figure (S_r) signifies a circle of radius r.

4 Likelihood function calculations

To analyse catalogues such as the two from California, we need to apply a stochastic model of the earthquake process which takes all possible interactions into account. In this paper we have applied essentially the same branching model of earthquake occurrence used earlier (I, II); this is a restricted version of the model of complete interaction. In particular, the function describing the interaction between earthquakes is taken to be uniform within each of several small time–distance intervals surrounding the main event. This type of

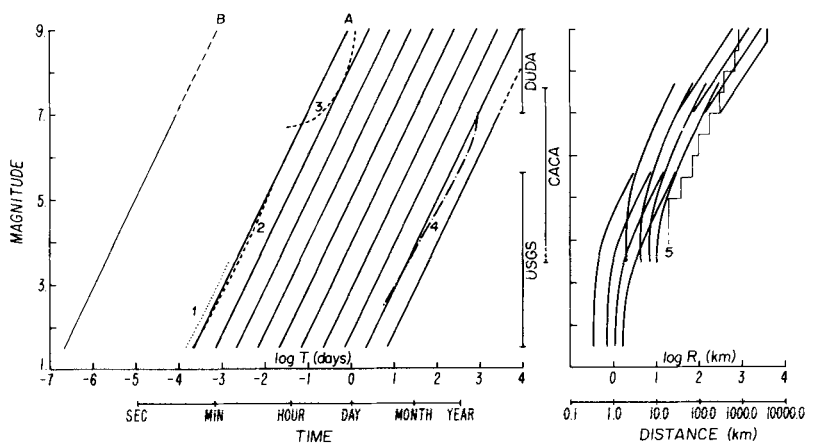

Figure 3. Time and distance intervals. The numbers are explained in the text. A is the estimate of signal duration of an earthquake, B is the estimate of rupture duration of an earthquake.

function has greater versatility in comparison with algebraic functions (I, p. 308). The time–distance plot around each earthquake was divided into nine time and four distance intervals, i.e. 36 space–time intervals both before and after the main event (Fig. 3). The equally-spaced parallel diagonal lines in the left-hand diagram of this figure show the boundaries of the time intervals as a function of magnitude of main event. Each of these intervals is sub-divided into four distance intervals as shown on the right side of the figure. We number the intervals of time sequentially from the shortest to the longest time interval, and number the intervals of distance similarly from the shortest to the longest range. We assume the magnitude distribution of dependent events varies as $c^{\Delta M}$, where c is an adjustable parameter in the fit and ΔM is the difference of magnitude between the main event and a dependent shock. Here, as in previous investigations, it is convenient to identify each 0.1 magnitude interval by an integer k

$$k_i = 10(M_i - M_{\text{cutoff}}) + 1.$$

The logarithmic likelihood function for the branching model may be calculated by the expression (equation (6) in I, equation (3) in II).

$$l = -A \cdot \frac{\gamma^{k_{\max}+1} - 1}{\gamma - 1} - \sum_{i=1}^{n} \sum_{s=1}^{4} \left(\sum_{t=1}^{9} \mu_{ts}^{-} \cdot \frac{c_{-}^{k_i} - c_{-}}{c_{-} - 1} + \sum_{t=1}^{9} \mu_{ts}^{+} \frac{c_{+}^{k_i} - c_{+}}{c_{+} - 1} \right)$$
$$+ \sum_{i=1}^{n} \log \frac{\nu(h_i)\, d\tau \cdot dh}{\Pi(H) \cdot T} + \sum_{i=1}^{n} \log \left[A \cdot \gamma^{k_i - 1} + \sum_{k_i < k_j} \mu_{ts} \cdot \frac{\Pi(H) \cdot T}{\Pi_j(\Delta H_s) \cdot \Delta T_t} \right] + \text{constant}\,(d\tau, dh). \tag{2}$$

In this equation the subscripts + and – refer to aftershocks and foreshocks respectively, t and s are the indices of the time and distance intervals, T is total time span of the catalogue, ΔT_t is the time span of the tth time interval, $\nu(h)$ is the level of seismicity of independent shocks, and $\Pi(\Delta H_s)$ is the average number of independent shocks in the sth ring around the main shock,

$$\Pi(A) = \int_A \nu(h)\, dh$$

and n is the total number of earthquakes in the 'inside' catalogue. A and γ correspond roughly to the parameters 'a' and 'b' in the magnitude frequency relations; and μ is the branching coefficient defining the number of dependent shocks per 0.1 magnitude interval.

The logarithm of the likelihood function for a Poissonian model of the process l_0 may be calculated by setting the value of the branching coefficients μ in equation (2) to be zero. Actually we are interested in the difference $(l - l_0)$ and for this quantity, the third and fifth terms in equation (2) are absent.

In order to intercompare the three catalogues some scaling must be applied. The differences in the principal magnitudes of shocks in each of the three catalogues means that the duration of aftershock sequences and the distances over which aftershocks might be expected to occur should be an increasing function of magnitude. Such a model was proposed by Knopoff & Gardner (1972) and Gardner & Knopoff (1974).

The determination of the appropriate distance–magnitude scaling law presents a difficult problem. For the smallest earthquakes in a catalogue, the size of the focal zone, or the zone where the shock influences the stress pattern, is much less than the error in locating the earthquakes. A similar problem arises when we use the epicentral, rather than the hypocentral, distance between the shocks, since depth estimates are much less accurate than

those for epicentral coordinates. Thus the details of the interaction pattern of the smallest earthquakes in a given catalogue are smoothed due to location errors. As noted above, the relative errors are of importance because we use the distances between events to compute the likelihood function; as a consequence, the average values of the standard errors in epicentre location should roughly define the distance interval scale for small shocks. For USGS these errors are 0.5–1.0 km; for CACA the errors are 1.5–4.0 km.

With regard to the upper magnitude limit of a catalogue, empirical magnitude–distance relations have been well studied (King & Knopoff 1968; Kanamori & Anderson 1975). A combination of the magnitude–fault length relation, together with the increasing importance of uncertainties in epicentre location at small magnitudes, has been considered by Knopoff & Gardner (1972) for the NOAA catalogue 1964–71 where it is assumed that the uncertainties in location overtake the distance–magnitude formula around $M = 5$. The Knopoff–Gardner (1972) relation, which is intended as an upper bound to isolate aftershock sequences, is shown in Fig. 3 as line 5. In this paper we use a similar relation with logarithmic subdivisions of the distance intervals as shown in Fig. 3. Several calculations have been made with different sets of parameters to define the intervals, and those shown in Fig. 3 have been found appropriate for this calculation by being close to the maximum of the likelihood function.

To define the magnitude–time scaling parameters (I, pp. 302–303), we have calculated the value of $l - l_0$ for different values of the scaling factor θ, which is defined so that if the magnitude of the main shock increases by one unit, the time interval is changed by a factor of θ, i.e. ΔT_t in equation (2) will be changed to $\Delta T_t \cdot \theta^{\Delta M}$ (see Fig. 3). For values of θ between 2.0 and 4.0 there is very little change in the likelihood function (I, p. 303); very likely this means that, for our model (equation (2)), θ is closely correlated with some of the other parameters and hence is ill-defined.

There are two alternative ways to compute the factor θ. In the first alternative we adjust the parameter θ to match the relationship between the duration of the earthquake signal and the magnitude of the shock. During a large earthquake it is difficult to determine arrival times of close aftershocks of the event; hence a catalogue is incomplete.

The data specifying the magnitude–signal duration dependence for small shallow earthquakes (Lee, Bennett & Meagher 1972a; Real & Teng 1973), plotted in Fig. 3 as lines 1 and 2 respectively, suggest that $\theta = 3.0$ would be appropriate for our purposes (see also Herrmann 1975). The long-period (M_S) data (Evernden 1976, p. 550) also support this value, though not so definitively. The durations in line 3 were calculated using an amplitude level corresponding to $M_S = 5.5$. This cutoff amplitude limit seems to be appropriate for the largest part of DUDA.

The second alternative uses a postulated relation between an upper bound for the duration of aftershock sequences and the magnitude of the main shock given by Gardner & Knopoff (1974) for earthquakes in Southern California; this curve is plotted in Fig. 3 as line 4 and also gives a value of $\theta = 3.0$. The corresponding curve from the NOAA list of worldwide earthquakes also gives the same value (Knopoff & Gardner 1972). The value $\theta = 3.0$ was used in our computations.

To avoid the inhomogeneities introduced into a catalogue at short times after a large event, we have deleted all earthquakes from the catalogues which lie to the left of line A in Fig. 3, which is our estimate of the duration of the earthquake signal. The number of earthquakes removed for the 'inside' USGS catalogue is 103 or about 2 per cent; for the CACA catalogue it is 160 or about 16 per cent and for the DUDA catalogue it is 20, also about 2 per cent. In Section 8 we discuss possible bias that might be introduced by such removal of close, dependent shocks.

5 Results

The values of the parameters obtained by maximizing the likelihood function of equation (2) and some characteristics of the catalogues are shown in Table 1. The estimates of errors were obtained by inversion of the matrix of second derivatives $\partial^2 l/\partial P_i \partial P_j$, where P_i is the ith parameter.

Table 1. Values of the parameters in the stochastic model.

Parameters	Catalogue		
	USGS	CACA	DUDA
$\gamma_0 (b_0)$	1.220 ± 0.003 (0.86)	1.225 ± 0.008 (0.88)	1.270 ± 0.011 (1.04)
α_0	375.0 ± 4.0	89.5 ± 2.5	57.0 ± 2.0
γ	1.224 ± 0.004	1.235 ± 0.012	1.263 ± 0.012
α	251.6 ± 4.6	46.0 ± 2.6	46.7 ± 2.5
$\Sigma\mu^-$	0.02025	0.02592	0.01119
$\Sigma\mu^+$	0.01834	0.01979	0.02365
$c_-(c_-^{10})$	0.936 ± 0.023 (0.51)	0.856 ± 0.078 (0.21)	1.003 ± 0.077 (1.03)
$c_+(c_+^{10})$	1.169 ± 0.006 (4.75)	1.188 ± 0.007 (5.66)	1.116 ± 0.045 (2.99)
ν_-	0.143	0.122	0.114
ν_+	0.477	0.575	0.453
N_- (per cent)	379.5 (6.8)	44.5 (5.3)	37.1 (4.2)
N_+ (per cent)	1432.1 (25.6)	363.8 (43.5)	137.8 (15.4)
M_{max}	5.2	7.7	8.9
M_{cutoff}	1.5	4.0 (3.5)	7.0
n	5586	837	894
$l_{max} - l_0$	4670.8	1665.3	145.4
I/n (bits)	1.21	2.87	0.23

We have the relation $b = 10 \log_{10}\gamma$ for independent earthquakes, and for the Poissonian model $b_0 = 10 \log_{10}\gamma_0$. The results show a slight increase of b_0 with M_{max}; this may reflect a weak non-linearity of the magnitude–frequency curve plot over the whole range of magnitudes or it might be due to our use of the different magnitude scales M_S and M_L (see end of Section 2). With regard to the parameter a in the magnitude–frequency law, we write this law in the form

$$\log_{10}\dot{N} = a - bM_r - b(M - M_r).$$

The usual value of the activity coefficient a corresponds to the reference magnitude $M_r = 0$. However, $M_r = 0$ is usually a magnitude outside the span encompassed by most catalogues. Hence the value of a is statistically correlated with values of b. A statistically independent estimate of $(a - bM_r)$ would be to take M_r near the 'centre of gravity' of the magnitude–frequency data. We have, for convenience used a value close to this, namely,

$$\alpha = a - b(M_{cutoff} + 0.5).$$

In other words, α is the ordinate at $M_r = M_{cutoff} + 0.5$. The parameter A in equation (2) is the ordinate at the upper magnitude limit of the catalogue.

The parameters (γ, α) describe the distribution of independent shocks for our branching model. The number of these shocks is significantly smaller in comparison with the Poissonian model. The parameters $\Sigma\mu^-$ and $\Sigma\mu^+$ describe dependent shocks: the former

gives the total number of foreshocks and the latter the number of aftershocks in the magnitude interval 0.1 unit, as the difference of magnitude between these shocks and the main event approaches zero. In the calculations we have not considered the interaction of earthquakes with equal integer magnitudes k but, if this interaction were taken into account, it would only increase the value of the likelihood function by about 3 per cent. The values of $\Sigma\mu^-$ and $\Sigma\mu^+$ are approximately equal for all three catalogues; it should be noted that we have used eight time intervals for DUDA instead of nine so we expect lower values for this catalogue. The quantities c_- and c_+ give the magnitude distributions of the foreshocks and aftershocks respectively (equation (2)). For example, the value of $c_-^{10} = 0.51$ means that for each change of one unit of magnitude, the number of foreshocks changes 0.51-fold. Once again there is great similarity among the c_+, c_- values for all three catalogues. The similarity of the $c_\pm$ and the $\mu_\pm$ values may be a fortuitous consequence of close correlation between estimates of these parameters; the correlation coefficient is of the order 0.1–0.4. Hence we have calculated the number of dependent shocks ν for a magnitude difference of one unit:

$$\nu = \frac{c^{11} - c}{c - 1} \cdot \Sigma\mu \tag{3}$$

and once again we have good agreement among all three catalogues. The N-values (Table 1) are the total number (and the percentage) of dependent shocks throughout the catalogue.

The c-values are significantly different with regard to the magnitude distribution of the fore- and aftershocks: there are many aftershocks which are much weaker than the main shock, while the number of foreshocks diminishes as the magnitude difference between the main shock and the foreshocks increases. It is interesting to note that $c_- \approx 1/c_+$ and $\Sigma\mu^- \approx \Sigma\mu^+$ for each catalogue. This means that in reality there are no strict differences between fore- and aftershocks; they are simply descriptions of the same mutual interaction of earthquakes. We discuss this notion further in the next section.

The last row of Table 1 gives the information rate per earthquake, i.e. how much information we can obtain about an earthquake, on the average, from a given catalogue, for this particular model of the earthquake process (this calculation uses base 2 logarithms); see II for more detail. This rate depends strongly on the magnitude span of the catalogue; another influence, as will be seen below, is the presence of a very strong earthquake in the catalogue. With the data presently at our disposal, we are able to obtain information about future earthquakes in the amount of 0.5 to 1.0 bits per shock, i.e. to reduce the uncertainty of the predicted event by a factor of $2^{0.5}$ to $2^{1.0}$ (II).

The similarity of earthquake processes in the different magnitude ranges is exemplified further by Table 2, which shows the time–distance interaction of earthquakes. Values of μ such as 10 ± 16 should not be taken to mean that μ can take on a negative value: by definition μ is non-negative. As noted in I, these $\pm$ values give only a crude estimate of uncertainty. Values of μ that are most reliable are those for times closest to the origin time of the main earthquake, i.e. corresponding to the smaller sequence numbers of time intervals. These estimates of μ are also less dependent on the specific assumptions regarding the model and these estimates are virtually uncorrelated statistically with the estimates of the other parameters than c, the values of these correlation coefficients are generally less than 0.1. The values of μ for longer time intervals, i.e. larger sequence numbers, show much larger scatter. Taking these observations into account, we assert that the values of μ are similar for all three catalogues. With increasing distance, the larger values of μ are found among the greater time intervals. This means that aftershocks are migrating with velocities of from 2 to 10 km/day at the beginning of the sequence and from 0.1 to 0.5 km/day for remote aftershocks. Foreshocks seem to move toward the main shock.

The time–distance interaction of earthquakes in different magnitude ranges can be investigated by constructing four-dimensional distributions, with the magnitude of the main event, the magnitude of the dependent event, the distance and the time as the variables. Indeed, by putting the values of the parameters we have already derived into the computational scheme, it is possible to calculate the number of dependent shocks in any given four-dimensional interval; this has all the advantages of the moment approach (see Section 3) and differs only in that all the major interactions will have been taken into account automatically. From this calculation we find, for example, that the strongest earthquakes in the California catalogues (especially in CACA) were not preceded by significant numbers of foreshocks; the non-zero values of μ corresponding to foreshocks, are connected mostly with earthquakes of small and medium size. This does not invalidate the concept of foreshocks as a common and frequent occurrence (I; Jones & Molnar 1976). In CACA there are only two major earthquakes, so the statistics are poor; DUDA gives many examples of strong earthquakes preceded by foreshocks. However, the annoying possibility exists that California may be anomalous in regard to the presence of foreshocks; we simply do not have sufficient data.

Another feature we have investigated is the behaviour of different sizes of aftershocks. For a specified time interval, we compared the numbers of aftershocks in the region that is most distant from the focal zone, distance intervals 3 and 4, with the total number of aftershocks; the latter number is the sum of the entries in the four distance intervals. The time intervals we have chosen are grouped by threes to increase the population in the entries. These ratios are shown in Table 3 for different magnitude ranges of main and dependent earthquakes. The values of $\Delta M = M_1 - M_2$ between the centres of each magnitude band are also listed; entries for the same values of ΔM with different values of M_1 are connected by braces.

Four significant observations can be made with regard to Table 3. These are (1) the increase in the percentages from left to right across the top row, which can be interpreted to mean that strong aftershocks, with $\Delta M = 0$, are concentrated close to the epicentre in the early part of the time sequence and later, large aftershocks begin to migrate into the regions more remote from the epicentre; (2) the decrease in the percentages from left to right across the bottom row, which can be interpreted as implying that weaker aftershocks do not appear in large numbers at long range and at short times after the parent event and indeed this number becomes even smaller at long range in later times; (3) the decrease in values from top to bottom in the last column implies that we find a greater percentage of the total large aftershock population than the small aftershock population at large distances and large times from a parent earthquake; (4) the rather close agreement between the two pairs of rows connected by braces which testifies to the stability of the analysis. Unfortunately the number of aftershocks with $M_2 > 3.5$ is too small to draw reliable conclusions regarding the extension of this pattern. Partial confirmation may also be seen in Table 2, where the μ-values for DUDA soon achieve a zero value at the epicentre (distance intervals 1 and 2), while the μ-values for USGS, with a much greater magnitude span, remain non-zero for all time.

Similar results are obtained when we replace the two values of c in equation (2) by 12 values, each c-parameter being assigned to a region consisting of 3×2 time–distance intervals (Fig. 1). The gain in the likelihood function for the three catalogues was 12.8, 11.2 and 2.2 respectively; for USGS and CACA the results are significant at a level greater than 98 per cent; the results for DUDA of course are not statistically significant.

From the analysis of the USGS data (Table 4), we see that the values of c for foreshocks are in general lower near the epicentre than farther away; for aftershocks, the pattern is

Table 2. Values of branching ratio μ.

Distance intervals	Catalogue	Foreshock time intervals								
		9	8	7	6	5	4	3	2	1
1	USGS	134 ± 58	67 ± 38	141 ± 40	153 ± 39	154 ± 37	203 ± 41	133 ± 32	78 ± 23	29 ± 14
	CACA	0	10 ± 112	146 ± 136	12 ± 113	179 ± 128	167 ± 125	217 ± 135	0	117 ± 91
	DUDA	–	0	0	0	0	88 ± 65	48 ± 47	47 ± 44	120 ± 74
	average	67	26	96	55	111	153	133	42	89
2	USGS	0	115 ± 51	44 ± 34	150 ± 41	82 ± 32	71 ± 25	51 ± 21	40 ± 16	76 ± 22
	CACA	0	40 ± 155	112 ± 111	38 ± 97	256 ± 167	4 ± 141	64 ± 82	145 ± 112	174 ± 115
	DUDA	–	0	0	0	0	75 ± 61	56 ± 47	82 ± 59	0
	average	0	52	52	63	113	50	57	89	83
3	USGS	14 ± 61	0	44 ± 33	54 ± 28	26 ± 19	35 ± 17	46 ± 20	16 ± 10	0
	CACA	0	0	0	110 ± 116	113 ± 145	103 ± 109	82 ± 116	58 ± 62	0
	DUDA	–	110 ± 312	0	0	0	7 ± 32	20 ± 32	27 ± 43	0
	average	7	37	15	55	46	48	49	34	0
4	USGS	0	26 ± 53	1 ± 31	12 ± 24	0	0	11 ± 10	5 ± 7	14 ± 10
	CACA	0	94 ± 145	4 ± 104	45 ± 150	153 ± 151	0	85 ± 89	64 ± 67	0
	DUDA	–	0	360 ± 337	0	0	0	29 ± 46	24 ± 33	26 ± 32
	average	0	40	122	19	51	0	42	31	13
$\Sigma\mu^-$	average	74	155	285	192	321	251	281	196	185

		Aftershock time intervals								
1	USGS	62 ± 10	65 ± 10	72 ± 12	85 ± 13	78 ± 13	127 ± 17	103 ± 16	86 ± 18	102 ± 22
	CACA	78 ± 23	111 ± 29	178 ± 39	91 ± 28	154 ± 39	90 ± 29	58 ± 27	57 ± 27	9 ± 29
	DUDA	86 ± 44	63 ± 38	141 ± 61	93 ± 49	122 ± 63	0	0	0	–
	average	75	80	130	90	118	72	54	48	56
2	USGS	32 ± 7	54 ± 10	48 ± 10	81 ± 13	121 ± 17	88 ± 15	108 ± 18	81 ± 21	58 ± 27
	CACA	56 ± 20	101 ± 29	163 ± 39	148 ± 40	77 ± 33	77 ± 31	127 ± 39	34 ± 30	10 ± 40
	DUDA	0	34 ± 32	30 ± 31	76 ± 46	19 ± 48	140 ± 78	0	51 ± 156	–
	average	29	63	80	102	72	102	78	55	34
3	USGS	11 ± 4	28 ± 7	8 ± 4	22 ± 7	25 ± 8	27 ± 10	28 ± 14	52 ± 20	51 ± 30
	CACA	23 ± 13	0	0	15 ± 13	45 ± 21	12 ± 17	58 ± 28	0	0
	DUDA	0	10 ± 17	11 ± 26	12 ± 34	63 ± 58	55 ± 82	2 ± 132	56 ± 233	–
	average	11	13	6	16	44	31	29	36	26
4	USGS	4 ± 2	6 ± 3	6 ± 4	13 ± 5	8 ± 6	9 ± 8	4 ± 13	44 ± 23	37 ± 32
	CACA	0	8 ± 9	26 ± 23	0	19 ± 16	31 ± 24	23 ± 33	0	100 ± 63
	DUDA	9 ± 17	10 ± 18	13 ± 25	14 ± 39	68 ± 73	119 ± 127	158 ± 197	910 ± 379	–
	average	4	8	15	9	32	53	62	318	69
$\Sigma\mu^+$	average	119	164	231	217	266	258	223	457	185

All values of μ should be multiplied by 10^{-5}.

Table 3. Percentages of aftershocks in distance intervals 3 and 4 in USGS.

Magnitude interval of main shock, M_1	Magnitude interval of aftershocks, M_2	$\Delta M = M_1 - M_2$	Time intervals 1–3	4–6	7–9
2.5 to 3.4	2.5 to 3.4	0	2.7	19.2	45.9
2.5 to 3.4	1.5 to 2.4	1	19.2	16.3	29.0
3.5 to 4.4	2.5 to 3.4	1	23.9	16.8	35.0
3.5 to 4.4	1.5 to 2.4	2	8.9	14.7	11.0
4.5 to 5.4	2.5 to 3.4	2	18.5	15.7	9.7
4.5 to 5.4	1.5 to 2.4	3	12.0	6.6	2.4

Table 4. Values of the coefficient c for catalogue USGS.

Distance intervals	Foreshock time intervals		
	1–3	4–6	7–9
1–2	0.727 ± 0.118	0.896 ± 0.039	0.989 ± 0.033
3–4	0.879 ± 2.165	0.915 ± 0.117	1.089 ± 0.054
	Aftershock time intervals		
	1–3	4–6	7–9
1–2	1.180 ± 0.010	1.169 ± 0.009	1.178 ± 0.018
3–4	1.173 ± 0.024	1.140 ± 0.028	1.031 ± 0.087

changed in the opposite sense. As indicated above, low values of c show the prevalence of strong dependent shocks and large values of c, their absence. Similar observations can be made for CACA aftershocks, but the pattern is not confirmed for CACA foreshocks. In any case the effect is small and its statistical reliability has not been fully tested. With these restrictions, we see that strong earthquakes are taking place at the site of the future main shock; after the main earthquake they migrate to the outer fringes of the focal area. In the focal area, weak shocks are suppressed before the main shock, but after the main shock the number of small shocks increases significantly. The changes of our parameter c correspond to changes of the b-value of the magnitude–frequency law before and after a strong earthquake (Wyss & Lee 1973). A low value of c corresponds to a decrease of the b-value, but this decrease depends also on the ratio of dependent to independent shocks in the sample. Near the time of the main shock when the rate of dependent shocks is high, the changes in b are great, etc.

6 Close interaction of shocks and pattern of earthquake occurrence

In the last row of Table 2 we give the sum over all distance intervals of the average values of the ratio μ. These values are roughly uniform over time. Since the time intervals we have used (Fig. 3) increase logarithmically, the rate of occurrence of dependent shocks increases as t^{-1} as we approach the time of the main shock. This is in fact the Omori law of aftershock occurrence (Richter 1958; Utsu 1969). A similar picture was obtained for foreshocks by Jones & Molnar (1976).

If we try to extrapolate these values of μ toward $t \to 0$ we will get an infinite number of foreshocks and aftershocks. Of course this is meaningless, since our notion of earthquakes as a point process, i.e. that earthquakes occur instantly at one point of the space, ceases to be valid as we approach the origin time of the earthquake. The duration and the dimensions of an earthquake are not infinitesimal. We can avoid this contradiction by assuming, for example, that the earthquake does not generate dependent shocks during the process of rupture. For reasonable estimates of the focal dimensions and velocity of rupture we get a rough estimate of the rupture duration shown as line B in Fig. 3. Those dependent events which take place in the time interval between lines A and B (Fig. 3) are not usually distinguishable (see also discussion in Section 4), but we may assume that their rate of occurrence increases continually with decreasing time interval to the origin time of the main shock. Recently there has been some discussion concerning these short-range multiple shocks (Trifunac 1972; Fukao & Furumoto 1975; Burdick & Mellman 1976).

Assuming the value of μ is constant in the interval between lines A and B, we can try to estimate the total number of aftershocks ν generated by the main shock and its aftershocks (Kagan 1973),

$$\nu = c\mu \frac{[c(1+\mu)]^k - 1}{c(1+\mu) - 1}. \tag{4}$$

Taking $c = 1.195$, and $\mu = 0.014$ we get for $\Delta M = 1.0$ the value $\nu = 0.46$; for $\Delta M = 2.0$ we get $\nu = 3.60$. From the relation $E \sim 10^{1.5M}$ we find that close aftershocks on the average have 10 per cent of the energy of the main shock, if the extrapolation of our model towards $t \to 0$ is valid. These estimates are approximate because we have not taken into account foreshocks and the possibility that a second-order aftershock, i.e. an aftershock of an aftershock, might fall outside the time interval. More exact calculations will be described in the next section.

The following picture of earthquake occurrence can be constructed. A forthcoming strong main shock suppresses the creation of small earthquakes in the future focal area; thus we have a decrease of seismic activity, or a seismic gap, before this earthquake. As the time of the main shock approaches, foreshocks migrate toward it and their rate of occurrence increases. The foreshocks are strong relative to the main shock. Finally one of them triggers an event which ruptures the entire focal region, thus becoming the main shock. Near the origin time there is actually a merger of foreshocks, main event and close aftershocks. During this time the c-value becomes larger than 1.0, reflecting the creation of many smaller earthquakes. Strong aftershocks soon migrate beyond the focal area, leaving behind mostly weaker earthquakes.

Unfortunately, the available data do not permit the evaluation of the pattern of earthquake occurrence in the time intervals far from strong earthquakes.

7 Monte Carlo simulation of an earthquake 'family'

As indicated above, we may use Monte Carlo techniques to estimate more precisely the number of close dependent events, which may occur during the main phase of an earthquake. For these calculations we have applied a continuum model of the interaction function between earthquakes, which is consistent with our results. The magnitude distribution of dependent shocks was taken to be $\exp(c\Delta M)$ and the rate of occurrence to be μt^{-1}. We take $c_- = -1.55, \mu^- = 0.0315, c_+ = 1.78, \mu^+ = 0.0205$; (these values are approximately equal to those obtained in Section 5). The total number of dependent shocks in the time interval between lines A and B (Fig. 3) was calculated both before and after $t = 0$;

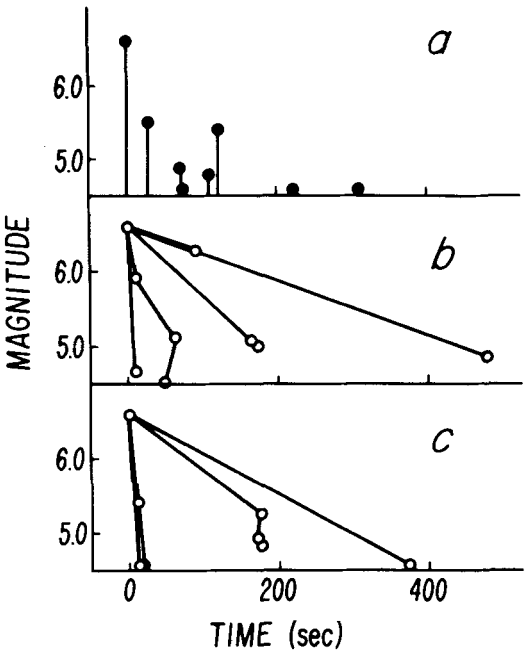

Figure 4. Magnitude–time plots of 1971 San Fernando earthquake sequences: (a) Actual sequence (Trifunac 1972), (b), (c) Monte Carlo simulations.

that is, both close foreshocks and aftershocks were taken into account. For $\Delta M = 1.0$ this number is equal to 0.59, and increases 7.5-fold for each increase of ΔM by one unit, in agreement with our previous calculation.

We can check to see if our conclusions that a shallow earthquake can be considered to be a multiple event (Miyamura *et al.* 1965) are compatible with the available data, i.e. is the extrapolation of our model toward $t = 0$ warranted? The most complete data for the time interval immediately after an earthquake are obtained from the accelerometer record of the 1971 San Fernando earthquake, during the first 6 min of the earthquake. Fig. 4(a) displays the time sequence for all shocks with $M \geqslant 4.5$ (Trifunac 1972) during this period. In Fig. 4(b) and (c) we show two examples of realizations of the aftershock sequence obtained by a Monte Carlo procedure using the values of parameters in the preceding paragraph. In addition, similar simulations may be made as a first step of generating synthetic seismograms. By averaging 2000 such realizations, we calculate that in only about 4 per cent of the cases, are seven or more aftershocks expected in this time interval; the average number of aftershocks is about 2.5. So we face the dilemma that either the 1971 earthquake was a relatively rare event, having seven aftershocks in 6 min, or the values of the parameters should be greater. Similar results can be obtained for the other major California earthquake, the 1940 Imperial Valley event (Trifunac & Brune 1970).

8 Monte Carlo simulations of catalogues

A similar simulation technique can be used to generate artificial catalogues of earthquake data (*cf.* Knopoff & Kagan 1977). Several problems are solved by creating the catalogues by Monte Carlo methods and then inverting them by the maximum likelihood method. Among these (1) we can test the general validity of our concepts and the computational scheme,

Table 5. Simulated California catalogues.

Number of realization	Number of events				
	Independent	Dependent		Total	Maximum magnitude
		All	Close		
1	318	217	89	535	6.7
2	336	889	382	1225	7.6
3	302	287	123	589	7.1
4	339	221	94	560	6.6
5	341	518	191	859	7.4

(2) we can estimate biases introduced by removing shocks at short time intervals or to simulate the absence of them in the catalogue and (3) we can evaluate the statistical errors associated with our estimates of the parameters.

To reduce computing time we restrict this calculation to one in a time–magnitude state space, i.e. we ignore the spatial distribution of the earthquakes. In its other details, the procedure was similar to that shown in Fig. 4, or to that described in II. To create a catalogue similar to CACA, earthquakes with magnitude 4.0 and greater were generated over a time span of 60 yr; the central 40 yr form the 'inside' catalogue. The interaction function was taken to be uniform over all 15 time intervals: nine of them are shown in Fig. 3 and the remaining six are located between lines A and B in Fig. 3; we take $\mu = 0.00260$, $c_+ = 1.17$, $c_- = 1/c_+$, $\gamma = 1.236$, $\alpha = 0.55$ earthquake/yr. These values are roughly equivalent to those obtained for CACA: α is the number of earthquakes with magnitude 4.5 ± 0.05. The principal results for five realizations of the 'inside' catalogue are given in Table 5. The number of independent shocks varies slightly, but the number of dependent shocks is strongly connected to the largest magnitude of the earthquake in the catalogue.

Table 6. The parameter values of simulated catalogue.

Parameters	Catalogue number					
	1*a*	1*b*	2*a*	2*b*	3*a*	3*b*
γ_0	1.285	1.290	1.240	1.235	1.265	1.270
α_0	33.5	28.0	80.8	55.9	38.0	29.9
γ	1.285	1.285	1.213	1.165	1.252	1.251
α	20.0	19.8	19.7	8.84	15.1	14.8
$\Sigma\mu^-$	0.03332	0.02154	0.03699	0.01990	0.04723	0.02974
$\Sigma\mu^+$	0.03856	0.02828	0.04139	0.02356	0.04249	0.03022
c_-	0.852	0.856	0.851	0.855	0.851	0.855
c_+	1.164	1.171	1.174	1.216	1.181	1.208
ν_-	0.153	0.101	0.169	0.093	0.216	0.139
ν_+	0.976	0.745	1.110	0.805	1.186	0.986
N_-	35.0	18.9	98.8	37.6	56.7	28.1
N_+	183.9	115.8	831.9	671.5	297.9	208.8
N_{ind}	316.1	311.3	294.3	133.9	234.4	229.1
$M_{\max}$	6.7	6.7	7.6	7.6	7.1	7.1
n	535	446	1225	843	589	466
$l_{\max} - l_0$	828.0	173.8	3568.0	756.3	1163.2	195.7
I/n (bits)	2.23	0.56	4.20	1.29	2.85	0.61

a – 15 time intervals, b – nine time intervals.

We have inverted the catalogue data to derive the values of parameters. A first round of calculation was made with a catalogue in its original form (column 'a' in Table 6) and a second round with the close dependent shocks removed (column 'b'). The first three catalogues in Table 5 were processed; the results are presented in Table 6 in a format compatible with that of Table 1. The parameters α and γ have a great deal of scatter, especially in case b, where the removal of close dependent shocks seems to cause an increase of c and to a lesser degree μ, so that the estimate of the number of independent shocks N_{ind} is drastically reduced. We propose that the close strong shocks which are removed are 'parents' of some of the remaining shocks, so these missing parents should be replaced by a greater 'productivity', as reflected in the values of the parameters μ and c of the remaining strong shocks. A closer investigation shows that the remote time intervals have the greatest change of the values of the parameters, up to 50 per cent; for closer intervals the bias is about 20 per cent. This may explain the slight increase of the average μ-values for larger time intervals (see rows $\Sigma\mu$ of Table 2). The estimates of parameters for 15 time intervals (case 'a') show a rather good agreement with the original values: $\bar{c}_+ = 1.173 \pm 0.00048$. The values of N_{ind} display the largest differences; these values are all less than the expected value of 332.5. This bias is probably due to our use of outside shocks (see Section 2); if we do not use outside shocks it will result in a negative bias for the estimates of the parameters c and μ. It is possible, of course, to make more exact calculations, as we did in II, taking into account all the time and distance intervals between the shocks and the edges of a catalogue, but this will not be done here.

The values of the likelihood function and the information rate show significant dependence on the maximum magnitude of the earthquake in the catalogue (Section 5). These values are in general lower than similar estimates for real catalogues (Table 1), reflecting the absence of spatial information in the simulated catalogues. The large difference between the values for cases 'a' and 'b' show once again (II) that most of the information in the catalogues is contained in interactions of close events.

9 Discussion and summary

A coherent quantitative pattern of earthquake occurrence has been derived from the statistical analysis of three catalogues of shallow earthquakes. This picture synthesizes most of the known results of the time–space–magnitude interaction of earthquakes: the seismic gaps before earthquakes, the migration of epicentres, the change of b-values before and after a strong earthquake, the increase in the rate of foreshock occurrence before strong shocks, the complexity of the earthquake source function, etc. It has also been shown that the earthquake process is uniform over a broad range of magnitudes, extending from $M = 1.5$ to the largest earthquakes.

We can use our results in two ways: the first is an extrapolation of the catalogue in time, i.e. seismic risk prediction as in (II). As we have shown, the catalogues of earthquakes now available supply us with about 0.5–1.0 bits of information per earthquake. It is possible that different models of earthquake occurrence may raise this value somewhat, but it is doubtful that substantial improvement is possible. To show what improvement we need, consider the following example. From the values of parameters listed in Table 1, we calculate, using the Poissonian model, that the average return period of an earthquake with magnitude $8.0 > M > 7.5$ is about 100 yr, in the part of California spanned by CACA. If we had 10 bits of information per earthquake, we could reduce the uncertainty by 2^{10} times, resulting in an uncertainty in the conditional return period of a little more than one month. If an information rate of 20 bits were available, the earthquake could be pinpointed with an accuracy of about one hour.

In order to make this improvement possible, the information content of the catalogue must be enlarged significantly. Since we cannot increase the duration span of catalogues, an alternative would be to expand the description of an earthquake source, which is given at present in terms of only one parameter, the magnitude, to a more complicated, multi-dimensional description which may involve retrieving the complex earthquake source-time function from seismographic records (Gilbert & Dziewonski 1975). Here our results relating to the interaction of close earthquakes might be of help by providing an estimate of the *a priori* distribution of dependent shocks. Hence, a modified stochastic theory of earthquake occurrence can, in principle, contribute to the solution of one of the major inverse problems of seismology, namely the retrieval of the complex earthquake moment tensor function from seismograms.

A second application is the extrapolation of our results toward the origin time of the main shock, by the simulation of the complex source model of an earthquake. The forward problem involves the construction of synthetic seismograms for strong earthquakes, where the stochastic interaction of shocks is taken into account. The implications for engineering seismology are obvious.

Acknowledgments

The authors with to thank W. M. K. Lee, J. Pfluke, M. Friedmann and B. A. Bolt for providing us with relevant catalogues. The authors appreciate useful comments received from D. Vere-Jones and K. Aki. This research was supported by Grant ENV76-01706 of the RANN programme of the National Science Foundation.

Publication Number 1697, Institute of Geophysics and Planetary Physics, University of California, Los Angeles, USA.

References

Allen, C. R., St Amand, P., Richter, C. F. & Nordquist, J. M., 1965. Relationship between seismicity and geologic structure in the Southern California region, *Bull. seism. Soc. Am.*, **55**, 753–797.

Bolt, B. A. & Miller, R. D., 1971. Seismicity of Northern and Central California, 1965–1969, *Bull. seism. Soc. Am.*, **61**, 1831–1847.

Bolt, B. A. & Miller, R. D., 1975. *Catalogue of earthquakes in Northern California and adjoining areas, 1 January 1910–31 December 1972,* 567 pages, Seismographic stations, University of California, Berkeley.

Burdick, L. J. & Mellman, G. R., 1976. Inversion of the body waves from the Borrego mountain earthquake to the source mechanism, *Bull. seism. Soc. Am.*, **66**, 1485–1499.

Duda, S. J., 1965. Secular seismic release in the circum-Pacific belt, *Tectonophys.*, **2**, 409–452.

Evernden, J. F., 1976. Study of seismic evasion, III, *Bull. seism. Soc. Am.*, **66**, 549–592.

Fukao, Y. & Furumoto, M., 1975. Foreshocks and multiple shocks of large earthquakes, *Phys. Earth planet. Int.*, **10**, 355–368.

Gardner, J. K. & Knopoff, L., 1974. Is the sequence of earthquakes in Southern California with aftershocks removed, Poissonian?, *Bull. seism. Soc. Am.*, **64**, 1363–1367.

Gilbert, F. & Dziewonski, A. M., 1975. An application of normal mode theory to the retrieval of structural parameters and source mechanisms from seismic spectra, *Phil. Trans. R. Soc. Lond. A*, **278**, 187–269.

Gutenberg, B., 1955. Seismograph stations in California, in *Earthquakes in Kern county, California during 1952,* pp. 153–156, California division of mines, Bulletin 171.

Herrmann, R. B., 1975. The use of duration as a measure of seismic moment and magnitude, *Bull. seism. Soc. Am.*, **65**, 899–914.

Hileman, J. A., Allen, C. R. & Nordquist, J. M., 1973. *Seismicity of the Southern California region, 1 January 1932 to 31 December 1972,* 490 pages, Seismological Laboratory, California Institute of Technology, Pasadena.

Jones, L. & Molnar, P., 1976. Frequency of foreshocks, *Nature*, **262**, 677–679.

Kagan, Y. Y., 1973. A probabilistic description of the seismic regime, *Izv. Acad. Sci. U.S.S.R., Phys. Solid Earth*, pp. 213–219 (English translation).

Kagan, Y. & Knopoff, L., 1976. Statistical search for non-random features of the seismicity of strong earthquakes. *Phys. Earth planet. Int.*, **12**, 291–318.

Kagan, Y. & Knopoff, L., 1977. Earthquake risk prediction as a stochastic process, *Phys. Earth planet. Int.*, **14**, 97–108.

Kanamori, H. & Anderson, D. L., 1975. Theoretical basis of some empirical relations in seismology, *Bull. seism. Soc. Am.*, **65**, 1073–1095.

King, C.-Y. & Knopoff, L., 1968. Stress drop in earthquakes, *Bull. seism. Soc. Am.*, **58**, 249–257.

Knopoff, L. & Gardner, J. K., 1969. Homogeneous catalogs of earthquakes, *Proc. Nat. Acad. Sci.*, **63**, 1051–1054.

Knopoff, L. & Gardner, J. K., 1972. Higher seismic activity during local night on the raw-world-wide earthquake catalogue, *Geophys. J. R. astr. Soc.*, **28**, 311–313.

Knopoff, L. & Kagan, Y., 1977. Analysis of the theory of extremes as applied to earthquake problems, *J. geophys. Res.*, **82**, 5647–5657.

Lee, W. H. K., Eaton, M. S. & Brabb, E. E., 1971. The earthquake sequence near Danville, California, 1970, *Bull. seism. Soc. Am.*, **61**, 1771–1794.

Lee, W. H. K., Bennett, R. E. & Meagher, K. L., 1972a. A method of estimating magnitude of local earthquakes from signal duration, *U.S. Geol. Surv., Open File Report*, 28 pages.

Lee, W. H. K., Meagher, K. L., Bennett, R. E. & Matamoros, E. E., 1972b. Catalog of earthquakes along the San Andreas fault system in Central California for the year 1971, *U.S. Geol. Surv., Open File Report*, 67 pages.

Lester, F. W., Kirkman, S. L. & Meagher, K. L., 1976. Catalog of earthquakes along San Andreas fault system in Central California, October–December, 1973, *U.S. Geol. Surv., Open File Report*, 37 pages.

Meyers, H. & von Hake, C. A., 1976. *Earthquake data file summary*, 56 pages. National Geophysical and Solar–Terrestrial Data Center, Boulder, Colorado.

Miyamura, S., Omote, S., Teisseyre, R. & Vesanen, E., 1965. Multiple shocks and earthquake series pattern, *Bull. int. Inst. Seism. earthq. Eng.*, **2**, 71–92.

Real, C. R. & Teng, T. L., 1973. Local Richter magnitude and total signal duration in Southern California, *Bull. seism. Soc. Am.*, **63**, 1809–1827.

Richter, C. F., 1955. Foreshocks and aftershocks, in *Earthquakes in Kern county, California during 1952*, pp. 177–198, California division of Mines, Bulletin 171, San Francisco.

Richter, C. F., 1958. *Elementary seismology*, 768 pages, W. H. Freeman & Company, San Francisco.

Trifunac, M. D., 1972. Stress estimates for the San Fernando, California earthquake of February 9, 1971: Main event and thirteen aftershocks, *Bull. seism. Soc. Am.*, **62**, 721–750.

Trifunac, M. D. & Brune, J. N., 1970. Complexity of energy release during the Imperial Valley, California, earthquake of 1940, *Bull. seism. Soc. Am.*, **60**, 137–160.

Utsu, T., 1969. Aftershocks and earthquake statistics (I), *J. Fac. Sci. Hokkaido Univ. Japan*, Ser. VII, **3**, 129–195.

Wesson, R. L. & Ellsworth, W. L., 1973. Seismicity preceding moderate earthquakes in California, *J. geophys. Res.*, **78**, 8527–8546.

Wyss, M. & Lee, W. H. K., 1973. Time variation of the average earthquake magnitude in Central California, in *Proceedings of the conference on tectonic problems of the San Andreas fault system*, pp. 24–42, Geological Sciences, XIII, School of Earth Sciences, Stanford University.